BCAM and LAMA5 Mediate the Recognition between Tumor Cells and the Endothelium in the Metastatic Spreading of KRAS Mutant Colorectal Cancer

UNIVERSITÀ DEGLI STUDI DI TORINO

BCAM and LAMA5 Mediate the Recognition between Tumor Cells and the Endothelium in the Metastatic Spreading of KRAS Mutant Colorectal Cancer

Alice Bartolini[1], Sabrina Cardaci[1], Simona Lamba[1], Daniele Oddo[1,2], Caterina Marchiò[3], Paola Cassoni[3], Carla Azzurra Amoreo[4], Giorgio Corti[1], Alessandro Testori[1], Federico Bussolino[1,2], Renata Pasqualini[5,6], Wadih Arap[5,7], Davide Corà[1,2], Federica Di Nicolantonio[1,2 †] and Serena Marchiò[1,2,5,6 †]

[1]Candiolo Cancer Institute-FPO, IRCCS, 10060 Candiolo (Turin), Italy; [2]Department of Oncology, University of Turin, 10060 Candiolo (Turin), Italy; [3]Department of Medical Sciences, University of Turin, 10126 Turin, Italy; [4]Department of Pathology, Regina Elena National Cancer Institute, 00144 Rome, Italy; [5]University of New Mexico Comprehensive Cancer Center, [6]Division of Molecular Medicine and [7]Division of Hematology/Oncology, Department of Internal Medicine, University of New Mexico, Albuquerque, NM 87131, USA

[†] equal contribution

Running title: BCAM in KRAS mutant metastatic CRC

Keywords: colorectal cancer, tumor microenvironment, metastasis, KRAS, BCAM, targeted therapy

Financial support: This study was supported by Intramural Grant 5 per mille 2008 MIUR from Fondazione Piemontese per la Ricerca sul Cancro (FPRC)-ONLUS to DC, FDN, and SM, and Grant Farmacogenomica 5 per mille 2009 MIUR from FPRC-ONLUS to FDN. Work in the authors' laboratories was also supported by Associazione Italiana per la Ricerca sul Cancro (AIRC, MFAG4847 to SM, MFAG11349 to FDN, and IG17707 to FDN), FPRC-ONLUS 5 per mille 2011 Ministero della Salute to FDN, and Fondo per la Ricerca Locale (ex 60%), University of Turin, 2014 to FDN.

Conflict of interest statement: the authors declare no conflict of interests

Corresponding authors: Serena Marchiò and Federica Di Nicolantonio, Department of Oncology, University of Torino, Sp. 142, Km 3.95, 10060 Candiolo (TO), Italy. Phone: +39-011-9933239; Fax: +39-011-9933524; e-mail: serena.marchio@unito.it; federica.dinicolantonio@unito.it

TRANSLATIONAL RELEVANCE

Patients with KRAS mutant colorectal cancer (CRC) have a poor prognosis and are unresponsive to EGFR-targeted therapies. Therefore, novel approaches are urgently needed to prevent or reduce the metastatic progression in this patient subset. In this work, we have identified BCAM and LAMA5 as an unrecognized molecular system in KRAS mutant hepatic metastasis from CRC. In this pathological setting, BCAM was overexpressed in tumor epithelial cells and in tumor microenvironment (TME), while its ligand LAMA5 was specifically overexpressed in TME blood vessels. Two BCAM-mimic peptides showed preclinical efficacy against hepatic colonization by human KRAS mutant CRC cells. Inhibition of BCAM/LAMA5 interaction abrogated adhesion of KRAS mutant CRC cells to endothelial cells, suggesting that this system may be important in tumor-TME recognition events causative of the metastatic spreading. Together, our findings indicate that BCAM-targeted agents may provide novel prevention and/or early intervention strategies for KRAS mutant CRC metastasizing to the liver.

ABSTRACT

Purpose: KRAS mutations confer adverse prognosis to CRC and no targeted therapies have shown efficacy in this patient subset. Paracrine, nongenetic events induced by KRAS mutant tumor cells are expected to result in specific deregulation and/or relocation of tumor microenvironment (TME) proteins, which in principle can be exploited as alternative therapeutic targets.

Experimental Design: A multimodal strategy combining *ex-vivo*/*in vitro* phage display screens with deep-sequencing and bioinformatics was applied to uncover TME-specific targets in KRAS mutant hepatic metastasis from CRC. Expression and localization of BCAM and LAMA5 were validated by immunohistochemistry in preclinical models of human hepatic metastasis and in a panel of human specimens (n=71). The anti-metastatic efficacy of two BCAM-mimic peptides was evaluated in mouse models. The role of BCAM in the interaction of KRAS mutant CRC cells with TME cells was investigated by adhesion assays.

Results: BCAM and LAMA5 were identified as molecular targets within both tumor cells and TME of KRAS mutant hepatic metastasis from CRC, where they were specifically overexpressed. Two BCAM-mimic peptides inhibited KRAS mutant hepatic metastasis in preclinical models. Genetic suppression and biochemical inhibition of either BCAM or LAMA5 impaired adhesion of KRAS mutant CRC cells specifically to endothelial cells while adhesion to pericytes and hepatocytes was unaffected.

Conclusions: These data show that the BCAM/LAMA5 system plays a functional role in the metastatic spreading of KRAS mutant CRC by mediating tumor-TME interactions, and as such represents a valuable therapeutic candidate for this large, currently untreatable patient group.

INTRODUCTION

Despite major efforts to develop innovative bio-drugs, colorectal cancer (CRC) still remains largely an incurable disease in the metastatic setting (1, 2). A paradigmatic example is represented by EGFR targeted therapies, to which 85-90% patients are unresponsive. A large body of prior work has shown that mutations in EGFR downstream effectors, such as KRAS (3), NRAS (4), BRAF (5), and PI3K (6), lead to a constitutive activation of the signaling pathway, thus bypassing a therapeutic block of the receptor. The presence of a mutant RAS (either KRAS or NRAS) in the tumor is now a clinically approved criterion of exclusion from EGFR-targeted regimens. Historical attempts to directly target KRAS (e.g. by farnesyl transferase inhibitors) have so far failed (7), although recent innovative approaches appear to be more promising, at least from initial preclinical data (8, 9). Targeting single effectors downstream to KRAS, such as PI3K or MEK, showed little or no efficacy in CRC (10, 11). Alternative treatments are clearly needed for CRC patients with KRAS mutant tumors.

In this work, we hypothesized that an unexplored strategy to tackle KRAS would be to target proteins in the TME of KRAS mutant metastatic CRC. To identify such molecular targets, we set up preclinical models of human hepatic metastasis by implanting human CRC cell lines carrying monoallelic KRAS mutations (12) into the livers of immuno-suppressed mice. We used phage-displayed random heptapeptide libraries to profile exhaustive proteomic signatures selectively associated with these genetically controlled metastatic models. Unexpectedly, within these signatures we identified and characterized the transmembrane glycoprotein basal cell adhesion molecule (BCAM) (13) as being specifically associated to both the tumor and TME of KRAS mutant hepatic metastases. BCAM is a cell adhesion protein originally identified in the Lutheran blood group system and circulating sickle red cells, and a receptor for laminin α5 (LAMA5) (14), the chain supporting many of the biological functions of laminin α5, β1, γ1 (LM-511) in endothelial basement membranes.

Here, we demonstrate that BCAM is specifically overexpressed both in preclinical and clinical KRAS mutant hepatic metastasis from CRC. We further show that inhibition of the BCAM/LAMA5 pathway

leads to impaired adhesion of CRC cells to vascular endothelial cells, with consequent reduction of metastatic growth. We therefore propose BCAM as a specific TME marker and therapeutic target in KRAS mutant hepatic metastasis from CRC.

MATERIALS AND METHODS

Peptides and cell lines

All the peptides [control (scrambled): SLSTSKLTVASSLDRG; pep-BCAM1: ASGLLSLTSTLY; pep-BCAM2: SSSLTLKVTSALSRDG] were from New England Peptides (Gardner, MA), provided with >95% purity. The LIM1215 parental cell line (15) was obtained from Prof. Robert Whitehead, Vanderbilt University, Nashville, TN, with permission from the Ludwig Institute for Cancer Research Ltd, New York, NY. The metastatic variant of HCT-116 cells (16), and SW-48 and LIM1215 cell lines isogenic for KRAS mutant alleles (G12V, G12D and G13D) have been described (12). To obtain fluorescent cells for *in vitro* experiments, each cell line was individually infected with a lentiviral vector based on pLVX-IRES-ZsGreen1 (Clontech, Mountain View, CA). Human umbilical cord endothelial cells (HUVECs) were extracted and cultured as described (17). Human brain vascular pericytes (HBVP) were from ScienceCell Research Laboratories (Carlsbad, CA). All other cell lines were from LGC-Promochem (Sesto San Giovanni, Italy) and were cultured in specific media and standard supplements (Sigma-Aldrich, Milan, Italy). All cells were proven negative for mycoplasma and characterized by proliferation, morphology evaluation, and multiplex short tandem repeat profiling.

Animal models

Experiments were approved by the Institutional Animal Care and Use Committee (IACUC) and by the Italian Ministry of Health. Six-week-old female CD1-nude mice were purchased from Charles River (Lecco, Italy). All surgical procedures were performed under deep general anesthesia by isoflurane inhalation. For intrahepatic transplantation, a midline incision was performed, the median lobule of the liver was gently exposed (18) and 5×10^6 suspended cells were injected. The wound was closed by a double suture, and each animal was given 0.1 mg caprofen (Rymadil®, Pfizer, Milan, Italy) in physiological solution to allow post-operative pain relief and rehydration. Ampicillin was administered for 5 days after surgery. For phage display screens, tumor-bearing mice were sacrificed as soon as the masses became visible and/or before appearance of any sign of distress. For pharmacological

studies, cells were admixed with either targeting or control peptide (100 μM) immediately before intrahepatic injection. Explanted livers were photographed with a PL-200 camera (Samsung Electronics, Milan, Italy) and external areas of metastatic masses were quantified with ImageJ (16).

Phage display

Tissues and cell lines were processed (16) and maintained in binding medium [Iscove's Modified Dulbecco's Medium (IMDM) supplemented with 2% fetal calf serum (FCS)] at 4°C for the duration of the experiments. 10^{10} transducing units of a X_7 (X = any amino acid) phage library (Ph.D.™-7 Phage Display Peptide Library Kit, New England Biolabs, Ipswich, MA) was added to 5×10^5 target cell suspensions in binding medium, and incubated for 4 h at 4°C (first round). For successive rounds, phage was first pre-adsorbed on control cells/tissues for 1 h at 4°C, and subsequently incubated with target or control for 2 h at 4°C. After 5 washes in binding medium, bound phage was recovered and amplified by infection of K91Kan *Escherichia coli* in log-phase. Phage particles were purified by precipitation in PEG-NaCl (polyethylene glycol-800 20%, NaCl 2%).

Deep-sequencing and bioinformatics analysis

Phage DNA was extracted in iodide buffer (10 mM Tris HCl pH 8.0, 1 mM EDTA, 4 M NaI). Multiplexing barcodes (Illumina, San Diego, CA) were inserted by PCR in each individual sample and amplicons were purified by gel extraction (QIAquick® Gel Extraction Kit, QIAGEN, Hilden, Germany). DNA was quantified with Quant-iT™ PicoGreen® dsDNA Assay Kit (Invitrogen/Life Technologies, Monza, Italy), and purified DNA samples were multiplexed and sequenced with an Illumina HiSeq2000 instrument. The derived 101-bp paired-end reads were first de-multiplexed to separate single samples; successively, inserts were extracted based on the known flanking regions to give 21-bp oligonucleotide sets that were finally translated into the corresponding heptapeptides. Each peptide set was subjected to a similarity analysis with the repertoire of annotated protein sequences contained in the Ensembl database (19) via custom Perl scripts. Output proteins were accepted only if they shared at least 5 matches with a complete 7 residue sequence. To extract only the extracellular or

transmembrane proteins, the output datasets were filtered by Gene Ontology_Cell Component (GO_CC) annotations through the DAVID Bioinformatics Resource Functional Annotation tool (20) with default settings. The complete list of BCAM-mimic peptides has been submitted to the BDB: Biopanning Data Bank (21) and is accessible with the Dataset ID #2970.

Human samples and mutational analysis of KRAS

Formalin-fixed paraffin-embedded (FFPE) specimens from CRC patients were collected by the Units of Surgical Oncology and Pathology at Candiolo Cancer Institute-IRCCS, Mauriziano and Molinette Hospitals (Turin, Italy). Collection and manipulation of human samples were approved by the Institutional Review Board (IRB). Informed written consent was obtained from each patient in accordance with the Declaration of Helsinki. Genomic DNA was purified with the QIAamp DNA FFPE Tissue Kit (QIAGEN). PCR primers (from Sigma-Aldrich) were designed to amplify the selected exon with products ~250 bp in length. PCRs were performed in 96-well formats in 25-µl reaction volumes, in the presence of 0.25 mM deoxynucleotides (dNTPs), 1 µM each primer, 6% dimethyl sulfoxide (DMSO), PCR buffer, 0.05 U/µl Platinum Taq (Invitrogen/Life Technologies), and with a touchdown PCR program (Peltier Thermocycler, PTC-200, MJ Research, Bio-Rad). Products were purified with AMPure (Agencourt Bioscience Corp., Beckman Coulter, Milan, Italy). Sequencing was carried out with the BigDye Terminator v3.1 Cycle Sequencing kit (Applied Biosystems, Foster City, CA), and products were purified with CleanSeq (Agencourt Bioscience, Beckman Coulter) and evaluated on a 3730 DNA Analyzer (Applied Biosystems). Traces were analyzed with Mutation Surveyor software package (SoftGenetics, State College, PA).

Histological procedures

Immunohistochemistry (IHC) was performed on 2-µm FFPE tissue sections. Briefly, after deparaffinization and rehydration, antigens were retrieved by incubating at sub-boiling temperature in Tris-EDTA pH 9.0, followed by peroxidase inactivation and blocking of endogenous biotin. Sections were stained with antibodies specific for BCAM (1:250, Abcam, Prodotti Gianni, Milan, Italy), LAMA5

(1:100, Millipore, Milan, Italy) and Ki67 (1:100, Thermo Scientific, Milan, Italy), diluted in Antibody Diluent with Background Reducing Components (Dako, Cernusco sul Naviglio, Italy) for 1.5 h at room temperature (RT). Visualization of the staining was performed with avidin-biotin-peroxidase 3,3'-diamino-benzidine (DAB, Dako REAL™ Detection System Peroxidase/DAB+, Rabbit/Mouse, Dako). Sections were counterstained with hematoxylin, dehydrated and mounted in xylene-based mounting medium (Richard-Allan Scientific™ Cytoseal™ XYL, Thermo Scientific). The Mallory's trichrome stain was performed with the Mallory Trichrome Special Stains kit (Bio-Optica, Milan, Italy). Visible images were acquired with an ICC50HD camera (Leica, Milan, Italy); all human samples were also scanned in an Aperio ScanScope ® XT System (Leica). DAB signal was isolated by color deconvolution and the positive areas were quantified with ImageJ.

***In vitro* assays**

For cell adhesion assays, HUVECs, HBPV or THLE-3 cells were seeded to confluence in replicate wells of 24-well plates. In a first set of experiments, fluorescent cells (5×10^4/well) were allowed to adhere in 5% CO_2 at 37°C for 30 minutes, in the presence of control peptide, pep-BCAM1 or pep-BCAM2 (100 μM), as well as of the specific antibodies against BCAM or LAMA5 (1 μg/mL). In a second set of experiments, fluorescent HCT-116m cells were silenced for the expression of BCAM by specific Trilencer-27 siRNA Knockdown Duplexes (OriGene, Tema Ricerca, Bologna, Italy) in Lipofectamin RNAiMAX reagent (Life Technology). At 72 h post-transfection, adhesion on HUVECs was assayed in 5% CO_2 at 37°C for 30 minutes. In both experimental settings, plates were successively washed three times with phosphate-buffered saline (PBS) and fixed in 4% paraformaldehyde-containing PBS for 10 minutes at RT. Adhered cells were photographed under a fluorescence microscope and cell nuclei were quantified with ImageJ.

Immunoblot

Proteins were extracted in lysis buffer [150 mM NaCl, 50 mM Tris pH 7.4, 1 mM phenylmethane sulfonylfluoride (PMSF) protease inhibitor cocktail, Sigma-Aldrich] supplemented with 1% Nonidet NP-

40, and were separated by SDS-PAGE (Mini-PROTEAN® TGX Gels 4-10%, Bio-Rad, Segrate, Italy) followed by blotting onto PVDF membranes (Trans-Blot® TurboTM Transfer Pack, Bio-Rad). The BCAM-specific antibody (Abcam) was used 1:1,000 overnight at 4°C. Detection of specific signals was performed with a peroxidase-conjugated secondary anti-rabbit antibody and revealed by enhanced chemi-luminescence (Western Lightning® Plus-ECL, PerkinElmer, Waltham, MA).

Retrotranscription and Real-time PCR

Total RNA was extracted in QIAzol Lysis Reagent, purified with the RNeasy kit (both Qiagen, Hilden, Germany) and quantified with a Nanodrop instrument (Thermo Scientifics). One microgram RNA was subjected to retrotranscription with the High-Capacity cDNA Reverse Transcription Kit, and amplified in Power SYBR® Green PCR Master Mix with a 7900HT Real-Time PCR System (all Applied Biosystems). BCAM expression was evaluated with the dCt method, normalized against 3 independent housekeeping genes (Hypoxanthine Phosphoribosyltransferase 1, HPRT1; Succinate dehydrogenase complex, subunit A, SDHA; TATA Box Binding Protein, TBP), and expressed as fold increase (2^ddCt) over the control (WT KRAS) for each cell line panel. The following primers were used for the Real-time PCR amplification: BCAM_FW, CCTTCAGGATGAGCAGGAG; BCAM_REV, CCACTCTGCAGCCATAGGT; HPRT1_FW, TCAGGCAGTATAATCCAAAGATGGT; HPRT1_REV: AGTCTGGCTTATATCCAACACTTCG; SDHA_FW: TGGGAACAAGAGGGCATCTG; SDHA_REV: CCACCACTGCATCAAATTCATG; TBP_FW: CACGAACCACGGCACTGATT; TBP_REV: TTTTCTTGCTGCCAGTCTGGAC.

Statistics

All the analyses were performed with the Prism 5 software (GraphPad, La Jolla, CA): two-tailed t-test (C.I. 95%) and Fisher's exact test were used to compare selected experimental points; asterisks indicate the following p-value ranges: *, $P < 0.05$; **, $P < 0.01$; ***, $P < 0.001$.

RESULTS

BCAM and LAMA5 are a candidate receptor/ligand system in KRAS mutant hepatic metastasis from CRC. To reproduce the molecular diversity at the tumor-TME interface in hepatic metastasis from CRC, we set up mouse models derived by intrahepatic implant of human CRC cell lines (SW-48 and LIM1215) in which a single KRAS allele had been replaced by either a WT or one of three mutant (G12D, G12V, G13D) KRAS coding sequences by site-specific recombination (12). Such cells recapitulate genetic events observed in patients and represent a more physiological model of CRC epithelial cells in comparison to mutant KRAS-overexpressing cells. In addition, we observed that both SW-48 and LIM1215 generate hepatic masses with a substantial TME component, making them suitable preclinical models of metastatic CRC. To identify TME markers in KRAS mutant hepatic metastasis, we designed a high-throughput proteomic approach based on low-stringency parallel screens of phage-displayed random heptapeptides on all the experimental metastases (*ex-vivo*) and cell lines (*in vitro*) (**Figure 1A**), each screen providing 10^4-10^6 unique heptapeptide ligands (**Supplemental Material**, details of the procedure; **Figure S1**, quality control). From these massive datasets, we derived heptapeptide ligands with dual specificity for (i) mutant KRAS [mutant *vs.* WT] and (ii) TME [experimental metastases (tumor cells + TME) *vs.* cell lines (tumor cells only)]. Corresponding native protein networks were reconstructed by high-stringency sequence identity analysis, leading to the identification of candidate TME-binding proteins for each KRAS mutant setting. Such proteins were assigned a TME score, based on the percent experimental points in which they had been identified (**Figure 1B**). By definition, a TME-binding protein is a receptor expressed by tumor and/or TME cells that binds TME-specific ligands. In the described *in vivo* models of hepatic metastasis, tumor and TME components are human and murine, respectively. On this basis, we refined our search on candidate receptors (i) associated with all three mutant KRAS settings, (ii) retrieved in both human (tumor epithelial cells) and mouse (TME) proteomes, and (iii) whose recognized ligand(s) was retrieved exclusively in the mouse proteome (TME). BCAM was identified as the only protein fulfilling all these criteria (**Figure 1C**).

BCAM and LAMA5 are overexpressed in KRAS mutant hepatic metastasis from CRC. As an initial step toward the characterization of these new candidate markers, we validated the levels and distribution of BCAM and LAMA5 in hepatic metastases with different KRAS mutational status. Tissues from the described mouse models were IHC-stained, revealing that BCAM was overexpressed in both epithelial cells and TME (stroma and vasculature) of KRAS mutant experimental metastases, compared to WT tumors where it was undetectable. Staining for LAMA5 was barely detectable in epithelial cells but strong in the TME of KRAS mutant tumors (**Figure 2**, upper panels). *In vitro*, BCAM protein amounts were consistent with those observed *in vivo*, with the exception of SW-48 WT and LIM1215 WT cell clones, which expressed BCAM at medium levels (**Figure S4A**). Overall, there was no correlation between protein and mRNA levels in cultured cell lines (**Figure S4B**). Together, these data suggest that *in vivo* protein levels are influenced by the microenvironment and are possibly regulated by post-transcriptional events related to the occurrence of a mutant KRAS gene in cancer cells.

We next evaluated the presence of BCAM and LAMA5 in hepatic metastases from CRC patients. Overexpression of BCAM and LAMA5 was confirmed in KRAS mutant metastases, with only a difference in the staining pattern compared to the mouse models: in human TME, BCAM and LAMA5 were confined to the vasculature and barely detectable in stromal cells (**Figure 2**, lower panels), a feature possibly related to the more organized and/or less inflammatory phenotype of clinical tumors compared to experimental models. BCAM expression was investigated in patient samples (n=29 WT and 42 KRAS mutant) also with a routine scanner set on default parameters (**Table 1**, patient cohort; **Figure 3A**, representative BCAM staining; **Figure S2**, complete panel). Although this cohort was relatively limited, our analysis confirmed BCAM overexpression in KRAS mutant *vs.* WT tumors ($P < 0.0001$, **Figure 3B**). The same approach was applied to a panel of primary CRCs (n=18 WT and 16 KRAS mutant, **Figure S3**), revealing a non-significant trend of increased BCAM expression in KRAS mutant *vs.* WT tumors (**Figure 3C**). In hepatic metastases from the same patients, however, this trend was highly significant ($P = 0.0098$, **Figure 3C**), suggesting that the overexpression of BCAM in KRAS

mutant tumors is specifically acquired or enhanced during the metastatic spreading.

These data show that increased levels of BCAM and LAMA5 are present in KRAS mutant hepatic metastases, and suggest BCAM-LAMA5 as a receptor-ligand system for targeted intervention.

BCAM-mimic peptides inhibit the intrahepatic growth of KRAS mutant human CRC cells. Several peptide sequences retrieved by phage display shared similarity with portions of both human and mouse BCAM (**Figure 4**, peptides used in this study; **Table S1**, complete list of BCAM-mimic peptides identified in the phage display screens). Most of them overlapped in two conserved regions, i.e. residues 212-223 (ASGLLSLTSTLY) and 504-519 (SSSLTLKVTSALSRDG) of the human protein, corresponding to portions of the immunoglobulin-like V-type 2 (also named D2) and C2-type 3 (D5) domains, respectively. Although the function of these phage display-identified portions of BCAM remains uncharacterized, both the D2-D3 linker and the D5 domain are required for LAMA5 binding (22, 23) (**Figure 4**). We therefore evaluated whether corresponding synthetic peptides could block any functional interaction involving BCAM in the experimental metastasis models.

Because both SW-48 and LIM1215 give rise to experimental metastases very slowly (SW-48, 72-127 days; LIM1215, 109-284 days) and with incomplete engraftment rates, we evaluated alternative human CRC-derived cell lines. Among the WT (n=7) and KRAS mutant (n=11) cell lines investigated, only HT-55 (WT), HCT-116m and DLD-1 (both mutant) were capable of producing experimental metastases in a relatively short period of time (28-35 days) and with high (75-100%) engraftment rates (**Table S2**). *In vitro*, these cells lines completely recapitulate the correlation between KRAS mutational status and BCAM expression levels observed in the isogenic xenograft models (**Figure S4A**, compare with **Figure 2**). For the *in vivo* pharmacological studies, each cell line was co-injected with either pep-BCAM1 (ASGLLSLTSTLY), pep-BCAM2 (SSSLTLKVTSALSRDG), or control peptide (100 μM each), and the ability to colonize the hepatic parenchyma was evaluated after 28 days on the explanted livers. When co-administered with the KRAS mutant cell lines, both pep-BCAM1 and pep-BCAM2 inhibited the occurrence and extent of experimental metastases compared to a control peptide. Neither peptide interfered with the engrafting of WT cells (**Figure 5**, **Figure S5**).

Together, these data demonstrate that BCAM-mimic peptides inhibit the intrahepatic growth of human CRC cells specifically in KRAS mutant settings where BCAM and LAMA5 are overexpressed.

BCAM drives the adhesion of KRAS mutant CRC cells to the vascular endothelium. There was no difference in the numbers of proliferating cells (evaluated by Ki67 staining) or the levels of BCAM (consistent with those observed in cultured cell lines, **Figure S4A**) and LAMA5 between pep-BCAM1, pep-BCAM2 or control peptide-treated experimental metastases (**Figure 3**). These data indicate that the BCAM-mimic peptides do not interfere with tumor growth rates or with BCAM/LAMA5 expression once the metastatic cascade has occurred. Rather, we hypothesized that an earlier step in metastatic progression of CRC, e.g. the recognition and/or binding between tumor epithelial cells and TME components, might be affected by the block of BCAM/LAMA5 binding.

To test this hypothesis, we investigated whether the BCAM-mimic peptides could inhibit the interaction of KRAS mutant cancer cells with cell types representative of the TME. For this purpose, we evaluated the adhesion of HCT-116m cells (the only cell line suitable for this assay, **Figure S6**) on human endothelial cells (HUVECs), pericytes (HBVP) and hepatocytes (THLE-3). For prompt visualization, HCT-116m were stably transduced with a lentiviral construct to express high amounts of a human codon-optimized variant of the reef coral *Zoanthus sp.* green fluorescent protein. HUVECs, HBPV and THLE-3 cells were seeded to confluence, and fluorescent HCT-116m cells were allowed to adhere in the presence of either control, pep-BCAM1 or pep-BCAM2 peptide, or in the presence of a specific anti-BCAM or anti-LAMA5 antibody. Targeted peptide- and antibody-treated HCT-116m cells showed substantially impaired adhesion on endothelial cells compared to the control, whereas adhesion on pericytes and hepatocytes was unaffected (**Figure 6A**). To confirm the role of BCAM in the interaction of CRC with endothelial cells, we silenced the corresponding gene with 3 different siRNA duplexes (**Figure 6B**). The down-modulation of BCAM also impaired adhesion of fluorescent HCT-116m to the endothelium (**Figure 6C**).

Collectively, these data strongly suggest a role for the BCAM/LAMA5 receptor-ligand interaction in the mutual recognition between CRC cells and the vascular endothelium.

DISCUSSION

Whilst anti-EGFR antibodies have prolonged survival in metastatic CRC (25), they have proven ineffective for 85-90% of patients (26) due to primary (e.g., related to RAS mutations) or secondary pharmacological resistance. Patient stratification according to mutational backgrounds (27) and drug combination to restrain the emergence of secondary resistance (28) may improve EGFR-targeted treatments, but not for patients with KRAS mutant tumors. Therapies that target the TME in addition to cancer cells should result in synergistic anti-tumor activity; such therapies are also expected to be less susceptible to development of resistance, because TME cells are genetically stable. However, the advantage of combining angiogenesis inhibitors with EGFR-targeted drugs has proven poor overall (29, 30), and absent in patients with KRAS mutant tumors (31). On the other hand, the availability of TME-targeting drugs other than angiogenesis inhibitors or immunomodulators remains disappointingly limited: a single agent addressed to cancer-associated fibroblasts (CAFs), sonidegib, has been approved by FDA for basal cell carcinoma (32), while a few others are undergoing preclinical evaluation in different tumor types including CRC (33, 34). The recent characterization of CAF-specific gene expression signatures in primary CRC (35, 36) may also be promising in the light of novel therapeutic strategies. Whether all these approaches would be translatable to patients with KRAS mutant tumors remains to be elucidated.

In KRAS mutant CRC, the tumor/TME crosstalk is altered, and specific molecules [among which EphA2 (37) in tumor cells, fascin-1 (38) and adrenomedullin (39) in the stroma] acquire a functional role, mediating cancer aggressiveness toward an accelerated metastatic spreading (40). Although pro-metastatic signaling pathways and signatures have been successfully identified in primary CRC, important players in the metastatic cascade might not be detectable in the primary tumor and should be sought in the actual TME of a secondary tumor. Taking all these points into consideration, we designed an approach aimed at the identification of molecular markers/pathways in the hepatic metastasis of KRAS mutant CRC, by the use of a clinically relevant mouse model that combines human KRAS mutant CRC cells with a murine TME. This system was explored by high-throughput

proteomics and deep-sequencing, to identify TME-binding proteins in KRAS mutant tumors. We focused our attention on the only receptor-ligand system that emerged from our high-stringency analysis, i.e. BCAM and LAMA5. Other players have as well been identified that might be worth of further characterization, among which laminin chains, Sema4A, integrins (α_8, α_x, β_5), Tie1, and Smoothened. The latter is a CAF-associated molecule targeted by sonidegib (30), confirming the reliability of our screening procedure and suggesting that this FDA-approved drug should be also explored in KRAS mutant CRC metastasizing to the liver.

BCAM and LAMA5 act at the interface between tumor cells and the TME, allowing a dual targeting of non-tumor and tumor components, which in principle should be more effective compared to standard combined therapies. Similarly, an allosteric inhibitor of IGF-1R (NT157) that acts both on tumor cells and CAFs by blocking IGF-1R/IRS1 and STAT3 signaling has showed preclinical efficacy in primary CRC (34). The uniqueness of BCAM and LAMA5, however, goes further: being a player in the tumor/vasculature crosstalk, this molecular system is likely involved in an early step of the metastatic cascade, i.e., the recognition between circulating CRC cells and hepatic sinusoids. We suggest a paracrine mechanism in which KRAS mutant CRC cells induce increased vascular levels of LAMA5 during metastatic colonization. In turn, high levels of LAMA5 would favor its interaction with BCAM on cancer cells, leading to their accumulation in sinusoids toward the metastatic colonization of the liver. Consistently, we demonstrated that blocking either BCAM or LAMA5 leads to impaired adhesion of CRC cells to the vascular endothelium, and inhibition of metastatic colonization.

The only curative approach against hepatic metastasis is surgery. However, ~50% of surgically-removed metastases relapse, possibly due to the spreading and growth of either single cells or micro-metastases that were already present but undetectable at the time of surgical intervention. This re-growth is favored by the pro-inflammatory environment elicited by the surgery itself, and takes places in a very limited period of time, ranging from a few minutes to a maximum of two weeks (41). We propose BCAM as an intervention target in a potential metastasis prevention scheme that targets KRAS mutant CRC cells disseminated to the liver in this postoperative inflammation phase. A similar

targeting of early metastatic phases has been proposed for the inhibition of Notch signaling (42), and we believe that these two approaches might be efficiently combined.

Interestingly, LAMA5 has a documented role in breast cancer cell migration and invasion (43), as well as in self-renewal of breast cancer stem cells (44). These studies are focused on laminin-integrin interactions; we suggest that similar functions of LAMA5 are possibly activated in metastatic CRC, where protein networks that include BCAM might be responsible for mechanisms that go beyond the simple tumor/TME recognition here described. Furthermore, because in hepatic metastasis BCAM is co-expressed with LAMA5 in vascular cells, additional autocrine mechanisms are possible, including a role in tumor angiogenesis. Although these aspects need further investigation, it is reasonable to hypothesize that a concomitant targeting of (i) cancer cell attachment to, and potentially invasion of the hepatic vasculature, (ii) sustenance of cancer stem cells, and/or (iii) angiogenesis would have a deep impact on the metastatic cascade, because it might be active also on established secondary tumors.

Finally, despite its characterization as adhesion protein in the Lutheran blood group system and circulating sickle red cells, BCAM has been shown upregulated in skin (45), brain (46), and endometrial-ovarian (47) tumors, in hepatocellular carcinoma (48), and in breast cancer (49), where it represents an independent marker of response to neoadjuvant chemotherapy (50). These data suggest that BCAM-targeted agents might have broad application in different tumor types besides the specific approach against KRAS mutant CRC metastasis described in the present work.

REFERENCES

1. Wagner JS, Adson MA, Van Heerden JA, Adson MH, Ilstrup DM. The natural history of hepatic metastases from colorectal cancer. A comparison with resective treatment. Ann Surg. 1984;199:502-508.

2. Siegel R, Desantis C, Jemal A. Colorectal cancer statistics, 2014. CA Cancer J Clin. 2014;64:104-117.

3. Lievre A, Bachet JB, Le Corre D, Boige V, Landi B, Emile JF, et al. KRAS mutation status is predictive of response to cetuximab therapy in colorectal cancer. Cancer Res. 2006;66:3992-3995.

4. Douillard JY, Oliner KS, Siena S, Tabernero J, Burkes R, Barugel M, et al. Panitumumab-FOLFOX4 treatment and RAS mutations in colorectal cancer. N Engl J Med. 2013;369:1023-1034.

5. Di Nicolantonio F, Martini M, Molinari F, Sartore-Bianchi A, Arena S, Saletti P, et al. Wild-type BRAF is required for response to panitumumab or cetuximab in metastatic colorectal cancer. J Clin Oncol. 2008;26:5705-5712.

6. Sartore-Bianchi A, Martini M, Molinari F, Veronese S, Nichelatti M, Artale S, et al. PIK3CA mutations in colorectal cancer are associated with clinical resistance to EGFR-targeted monoclonal antibodies. Cancer Res. 2009;69:1851-1857.

7. Cox AD, Der CJ. Ras history: The saga continues. Small GTPases. 2010;1:2-27.

8. Zimmermann G, Papke B, Ismail S, Vartak N, Chandra A, Hoffmann M, et al. Small molecule inhibition of the KRAS-PDEδ interaction impairs oncogenic KRAS signalling. Nature. 2013;497:638-642.

9. Ostrem JM, Peters U, Sos ML, Wells JA, Shokat KM. K-Ras(G12C) inhibitors allosterically control GTP affinity and effector interactions. Nature. 2013;503:548-551.

10. Adjei AA, Cohen RB, Franklin W, Morris C, Wilson D, Molina JR, et al. Phase I pharmacokinetic and pharmacodynamic study of the oral, small-molecule mitogen-activated protein kinase kinase 1/2

inhibitor AZD6244 (ARRY-142886) in patients with advanced cancers. J Clin Oncol. 2008;26:2139-2146.

11. Ganesan P, Janku F, Naing A, Hong DS, Tsimberidou AM, Falchook GS, et al. Target-based therapeutic matching in early-phase clinical trials in patients with advanced colorectal cancer and PIK3CA mutations. Mol Cancer Ther. 2013. 12:2857-2863

12. Di Nicolantonio F, Arena S, Gallicchio M, Zecchin D, Martini M, Flonta SE, et al. Replacement of normal with mutant alleles in the genome of normal human cells unveils mutation-specific drug responses. Proc Natl Acad Sci U S A. 2008;105:20864-20869.

13. Campbell IG, Foulkes WD, Senger G, Trowsdale J, Garin-Chesa P, Rettig WJ. Molecular cloning of the B-CAM cell surface glycoprotein of epithelial cancers: a novel member of the immunoglobulin superfamily. Cancer Res. 1994;54:5761-5765.

14. Udani M, Zen Q, Cottman M, Leonard N, Jefferson S, Daymont C, et al. Basal cell adhesion molecule/lutheran protein. The receptor critical for sickle cell adhesion to laminin. J Clin Invest. 1998;101:2550-2558.

15. Whitehead RH, Macrae FA, St John DJ, Ma J. A colon cancer cell line (LIM1215) derived from a patient with inherited nonpolyposis colorectal cancer. J Natl Cancer Inst. 1985;74:759-765.

16. Marchiò S, Soster M, Cardaci S, Muratore A, Bartolini A, Barone V, et al. A complex of alpha6 integrin and E-cadherin drives liver metastasis of colorectal cancer cells through hepatic angiopoietin-like 6. EMBO Mol Med. 2012;4:1156-1175.

17. Jaffe EA, Nachman RL, Becker CG, Minick CR. Culture of human endothelial cells derived from umbilical veins. Identification by morphologic and immunologic criteria. J Clin Invest. 1973;52:2745-2756.

18. Kuo TH, Kubota T, Watanabe M, Furukawa T, Teramoto T, Ishibiki K, et al. Liver colonization competence governs colon cancer metastasis. Proc Natl Acad Sci U S A. 1995;92:12085-12089.

19. Flicek P, Amode MR, Barrell D, Beal K, Brent S, Carvalho-Silva D, et al. Ensembl 2012. Nucl Acids Res. 2012;40:D84-90.

20. Huang da W, Sherman BT, Zheng X, Yang J, Imamichi T, Stephens R, et al. Extracting biological meaning from large gene lists with DAVID. Curr Protoc Bioinformatics. 2009;13:13 1.

21. He B, Chai G, Duan Y, Yan Z, Qiu L, Zhang H, et al. BDB: biopanning data bank. Nucleic Acids Res. 2016;44:D1127-1132.

22. Mankelow TJ, Burton N, Stefansdottir FO, Spring FA, Parsons SF, Pedersen JS, et al. The Laminin 511/521-binding site on the Lutheran blood group glycoprotein is located at the flexible junction of Ig domains 2 and 3. Blood. 2007;110:3398-3406.

23. Zen Q, Cottman M, Truskey G, Fraser R, Telen MJ. Critical factors in basal cell adhesion molecule/lutheran-mediated adhesion to laminin. J Biol Chem. 1999;274:728-734.

24. Kikkawa Y, Ogawa T, Sudo R, Yamada Y, Katagiri F, Hozumi K, et al. The lutheran/basal cell adhesion molecule promotes tumor cell migration by modulating integrin-mediated cell attachment to laminin-511 protein. J Biol Chem. 2013;288:30990-31001.

25. Feng QY, Wei Y, Chen JW, Chang WJ, Ye LC, Zhu DX, et al. Anti-EGFR and anti-VEGF agents: important targeted therapies of colorectal liver metastases. World J Gastroenterol. 2014;20:4263-4275.

26. Van Cutsem E, Peeters M, Siena S, Humblet Y, Hendlisz A, Neyns B, et al. Open-label phase III trial of panitumumab plus best supportive care compared with best supportive care alone in patients with chemotherapy-refractory metastatic colorectal cancer. J Clin Oncol. 2007;25:1658-1664.

27. Dienstmann R, Salazar R, Tabernero J. Personalizing colon cancer adjuvant therapy: selecting optimal treatments for individual patients. J Clin Oncol. 2015;33:1787-1796.

28. Misale S, Bozic I, Tong J, Peraza-Penton A, Lallo A, Baldi F, et al. Vertical suppression of the EGFR pathway prevents onset of resistance in colorectal cancers. Nat Comm. 2015;6:8305.

29. Lv Y, Yang Z, Zhao L, Zhao S, Han J, Zheng L. The efficacy and safety of adding bevacizumab to cetuximab- or panitumumab-based therapy in the treatment of patients with metastatic colorectal cancer (mCRC): a meta-analysis from randomized control trials. Int J Clin Exp Med. 2015;8:334-345.

30. Larsen FO, Pfeiffer P, Nielsen D, Skougaard K, Qvortrup C, Vistisen K, et al. Bevacizumab in combination with cetuximab and irinotecan after failure of cetuximab and irinotecan in patients with metastatic colorectal cancer. Acta Oncol. 2011;50:574-577.

31. Do K, Cao L, Kang Z, Turkbey B, Lindenberg ML, Larkins E, et al. A Phase II Study of Sorafenib Combined With Cetuximab in EGFR-Expressing, KRAS-Mutated Metastatic Colorectal Cancer. Clin Colorectal Cancer. 2015;14:154-161.

32. 2015. Hedgehog Inhibitor Approved for BCC. Cancer Discovery.5:1011.

33. Wu Y, Cain-Hom C, Choy L, Hagenbeek TJ, de Leon GP, Chen Y, et al. Therapeutic antibody targeting of individual Notch receptors. Nature. 2010;464:1052-1057.

34. Sanchez-Lopez E, Flashner-Abramson E, Shalapour S, Zhong Z, Taniguchi K, Levitzki A, et al. Targeting colorectal cancer via its microenvironment by inhibiting IGF-1 receptor-insulin receptor substrate and STAT3 signaling. Oncogene. 2015. doi: 10.1038/onc.2015.326. [Epub ahead of print]

35. Calon A, Lonardo E, Berenguer-Llergo A, Espinet E, Hernando-Momblona X, Iglesias M, et al. Stromal gene expression defines poor-prognosis subtypes in colorectal cancer. Nat Genet. 2014;47:320-329.

36. Isella C, Terrasi A, Bellomo SE, Petti C, Galatola G, Muratore A, et al. Stromal contribution to the colorectal cancer transcriptome. Nat Genet. 2015;47:312-319.

37. Dunne PD, Dasgupta S, Blayney J, McArt DG, Redmond KL, Weir JA, et al. EphA2 expression is a key driver of migration and invasion and a poor prognostic marker in colorectal cancer. Clin Cancer Res. 2015;22:230-242.

38. Adams JC. Fascin-1 as a biomarker and prospective therapeutic target in colorectal cancer. Expert Rev Molecular Diagnostics. 2015;15:41-48.

39. Wang L, Gala M, Yamamoto M, Pino MS, Kikuchi H, Shue DS, et al. Adrenomedullin is a therapeutic target in colorectal cancer. Int J Cancer. 2014;134:2041-2050.

40. Nash GM, Gimbel M, Shia J, Nathanson DR, Ndubuisi MI, Zeng ZS, et al. KRAS mutation correlates with accelerated metastatic progression in patients with colorectal liver metastases. Ann Surg Oncol. 2010;17:572-578.

41. Taketo MM. Reflections on the spread of metastasis to cancer prevention. Cancer Prev Res. 2011;4:324-328.

42. Sonoshita M, Aoki M, Fuwa H, Aoki K, Hosogi H, Sakai Y, et al. Suppression of colon cancer metastasis by Aes through inhibition of Notch signaling. Cancer Cell. 2011;19:125-137.

43. Kusuma N, Denoyer D, Eble JA, Redvers RP, Parker BS, Pelzer R, et al. Integrin-dependent response to laminin-511 regulates breast tumor cell invasion and metastasis. Int J Cancer. 2012;130:555-566.

44. Chang C, Goel HL, Gao H, Pursell B, Shultz LD, Greiner DL, et al. A laminin 511 matrix is regulated by TAZ and functions as the ligand for the alpha6Bbeta1 integrin to sustain breast cancer stem cells. Genes Dev. 2015;29:1-6.

45. Schon M, Klein CE, Hogenkamp V, Kaufmann R, Wienrich BG, Schon MP. Basal-cell adhesion molecule (B-CAM) is induced in epithelial skin tumors and inflammatory epidermis, and is expressed at cell-cell and cell-substrate contact sites. J Invest Dermatol. 2000;115:1047-1053.

46. Boado RJ, Li JY, Pardridge WM. Selective Lutheran glycoprotein gene expression at the blood-brain barrier in normal brain and in human brain tumors. J Cereb Blood Flow Metab. 2000;20:1096-1102.

47. Planagumà J, Liljestrom M, Alameda F, Butzow R, Virtanen I, Reventos J, et al. Matrix metalloproteinase-2 and matrix metalloproteinase-9 codistribute with transcription factors RUNX1/AML1 and ETV5/ERM at the invasive front of endometrial and ovarian carcinoma. Hum Pathol. 2013;42:57-67.

48. Kikkawa Y, Sudo R, Kon J, Mizuguchi T, Nomizu M, Hirata K, et al. Laminin alpha 5 mediates ectopic adhesion of hepatocellular carcinoma through integrins and/or Lutheran/basal cell adhesion molecule. Exp Cell Res. 2008;314:2579-2590.

49. Rust S, Guillard S, Sachsenmeier K, Hay C, Davidson M, Karlsson A, et al. Combining phenotypic and proteomic approaches to identify membrane targets in a 'triple negative' breast cancer cell type. Mol Cancer. 2013;12:11.

50. Witkiewicz AK, Balaji U, Knudsen ES. Systematically defining single-gene determinants of response to neoadjuvant chemotherapy reveals specific biomarkers. Clin Cancer Res. 2014;20:4837-4838.

TABLES

Table 1. Patient cohort analyzed

	Category	Number	Percent
Sex	M	47/71	66.2%
	F	24/71	33.8%
Age at diagnosis	Mean	63	NA
	Median	65	NA
	>60-y old	42/71	59.2%
	<60-y old	29/71	40.8%
Primary tumor grade at diagnosis*	T1	3/68	4.4%
	T2	5/68	7.4%
	T3	39/68	57.3%
	T4	21/68	30.4%
Lymph node involvement at diagnosis*	Y	49/68	72.1%
	N	19/68	27.9%
Metastasis presentation	Synchronous	33/71	46.5%
	Metachronous	38/71	53.5%
KRAS status	WT	29/71	40.8%
	Mutant	42/71	59.2%

* staging unavailable for 3/71 patients

FIGURE LEGENDS

Figure 1. Identification of BCAM as a candidate receptor at the interface between tumor and TME in KRAS mutant hepatic metastases. (A) Experimental design: for each cell line, two WT or mutant (G12D, G12V, or G13D) KRAS clones were individually screened with a phage display library *in vitro* (cell culture) or *ex-vivo* (explanted tissues from the intrahepatic mouse models). For each condition, the phage display screens provided 5 experimental points (details in **Suppl. Methods**). (**B**) **Data analysis flowchart**: phage DNAs extracted from a total of 120 experimental points were deep-sequenced. Phage-displayed heptapeptides were inferred from all sequenced 21-bp oligonucleotide inserts and were subjected to BLAST analysis. Proteins with regions identical to at least 5 heptapeptides were scored based on their enrichment in mutant KRAS and *ex-vivo* experimental points, compared to WT and *in vitro*. (**C**) **Graph**, TME scores for human proteins retrieved in at least two, or in all three KRAS mutant settings. Scores are the mean of the 3 KRAS mutant settings. **Table**, TME scores (both human and mouse) for BCAM and LAMA5 in each mutant KRAS setting.

Figure 2. BCAM and LAMA5 are similarly overexpressed in KRAS mutant experimental metastases and patient specimens. 2-µm FFPE sections of (i) experimental metastases from intrahepatic implant of isogenic SW-48 cells in immuno-suppressed mice and (ii) surgically removed human liver metastases were stained with specific anti-BCAM and anti-LAMA5 antibodies and counterstained with hematoxylin. Images were acquired with a microscope-connected digital camera; representative pictures of KRAS mutant or WT tumors are shown. Black arrows, blood vessels; red arrows, stroma. BCAM and LAMA5, human proteins; Bcam and Lama5, mouse proteins.

Figure 3. BCAM overexpression is associated with KRAS mutant tumors in clinical settings. (**A**) BCAM expression in representative human samples (n=10 WT and 10 mutant KRAS) of liver metastasis. 2-µm FFPE tissue sections were stained for BCAM with routine hospital protocols and counterstained with hematoxylin. Images were acquired with an Aperio microscope-connected scanner set on default settings. (**B**) Quantitative evaluation of BCAM expression in the complete panel

of human samples (n=29 WT and 42 mutant KRAS). (**C**) Quantitative evaluation of BCAM expression in a subset (n=18 WT and 16 mutant KRAS) of matched primary CRCs and hepatic metastases. In **B** and **C**, DAB signals were isolated by deconvolution and quantified with ImageJ, and are expressed as percent positive area. ***, $P < 0.0001$; **, $P < 0.01$

Figure 4. Human BCAM protein structure and BCAM-mimic peptides. Schematic illustration of BCAM (i) domains, (ii) regions described as involved in the interaction with LAMA5, and (iii) regions identical to the phage display-identified peptides. For each peptide, the numbers of identity matches and of experimental points in which the sequence has been retrieved are indicated in parenthesis.

Figure 5. BCAM-mimic synthetic peptides inhibit the intrahepatic growth of human KRAS mutant CRC cells. Human CRC cell lines with WT (HT-55) or mutant (HCT-116m, DLD-1) KRAS (5×10^6 cells/mouse) were injected into the livers of immuno-suppressed mice (n=6-12), in the presence of either control or BCAM-mimic (pep-BCAM1, pep-BCAM2) peptides (100 μm each). Twenty-eight days after the implant, animals were sacrificed, and their livers were explanted and photographed for quantification of external tumor areas. Depending on the number of mice/group, differences between experimental points were evaluated by t-test or Fisher's exact test. FFPE tissue sections were subjected to Mallory's trichrome stain or immunostained with specific anti-Ki67, anti-BCAM and anti-LAMA5 antibodies, followed by counterstaining with hematoxylin. Representative pictures from one mouse/group are shown. BCAM and LAMA5, human proteins; Bcam and Lama5, mouse proteins. **, $P < 0.01$; *, $P < 0.05$

Figure 6. BCAM and LAMA5 mediate the adherence of KRAS mutant CRC cells to the vascular endothelium. (**A**) Fluorescent HTC-116m cells (5×10^4/well) were subjected to adhesion assays on confluent layers of endothelial cells (HUVECs), pericytes (HBVP) or hepatocytes (THLE-3), in the presence of (i) control, pep-BCAM1 or pep-BCAM2 peptide, or (ii) specific anti-BCAM or anti-LAMA5 antibody. Adhered cells were revealed and counted under a fluorescence microscope. Fluorescent HCT-116m cells were silenced for BCAM expression with 3 different siRNA duplexes (**B**) and

subjected to adhesion assays on HUVECs (**C**). Graphs indicate mean ± S.D. of sextuplicate wells and differences between samples were evaluated by t-test. ***, $P < 0.001$

Bartolini et al_Fig1

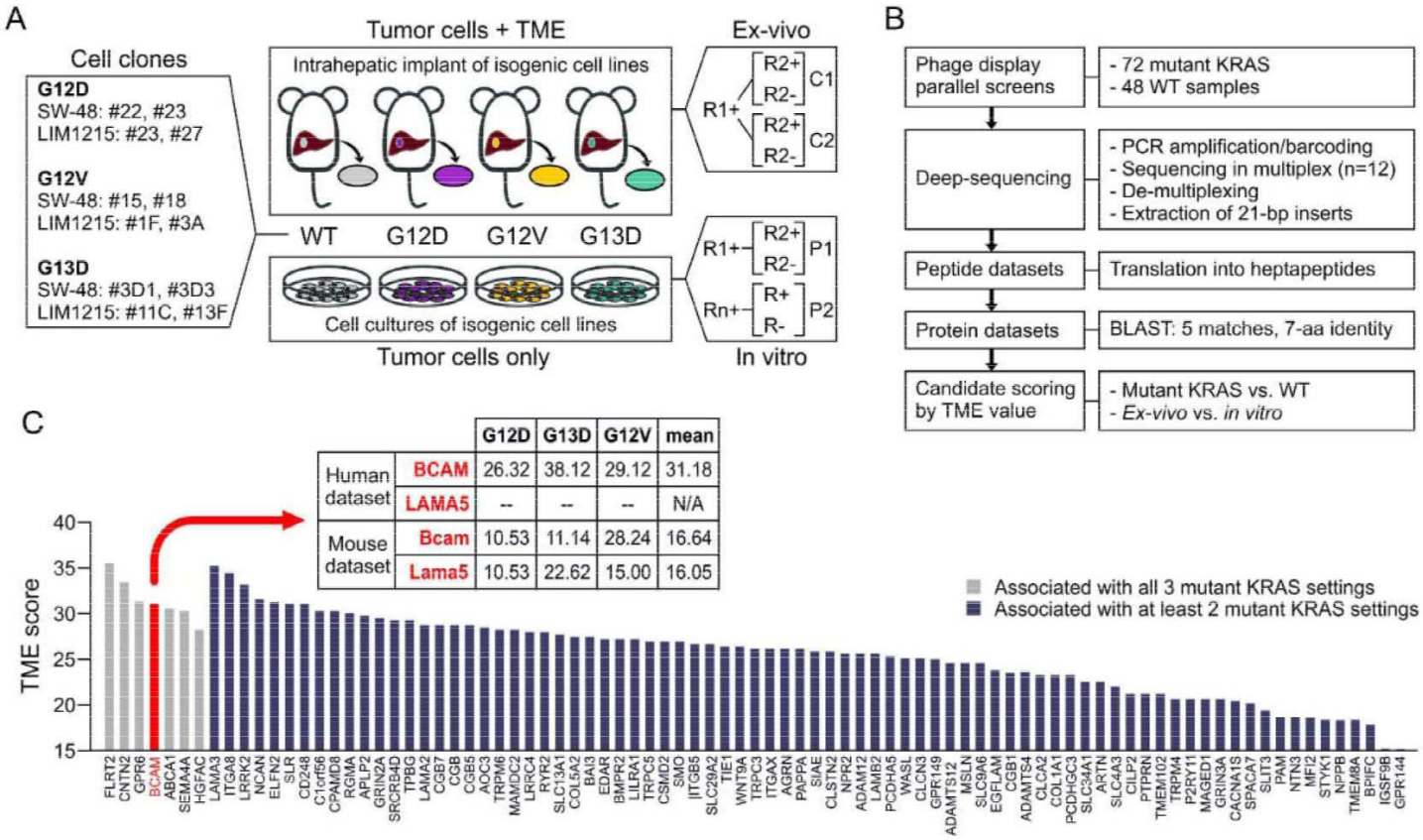

		G12D	G13D	G12V	mean
Human dataset	BCAM	26.32	38.12	29.12	31.18
	LAMA5	--	--	--	N/A
Mouse dataset	Bcam	10.53	11.14	28.24	16.64
	Lama5	10.53	22.62	15.00	16.05

Bartolini et al_Fig2

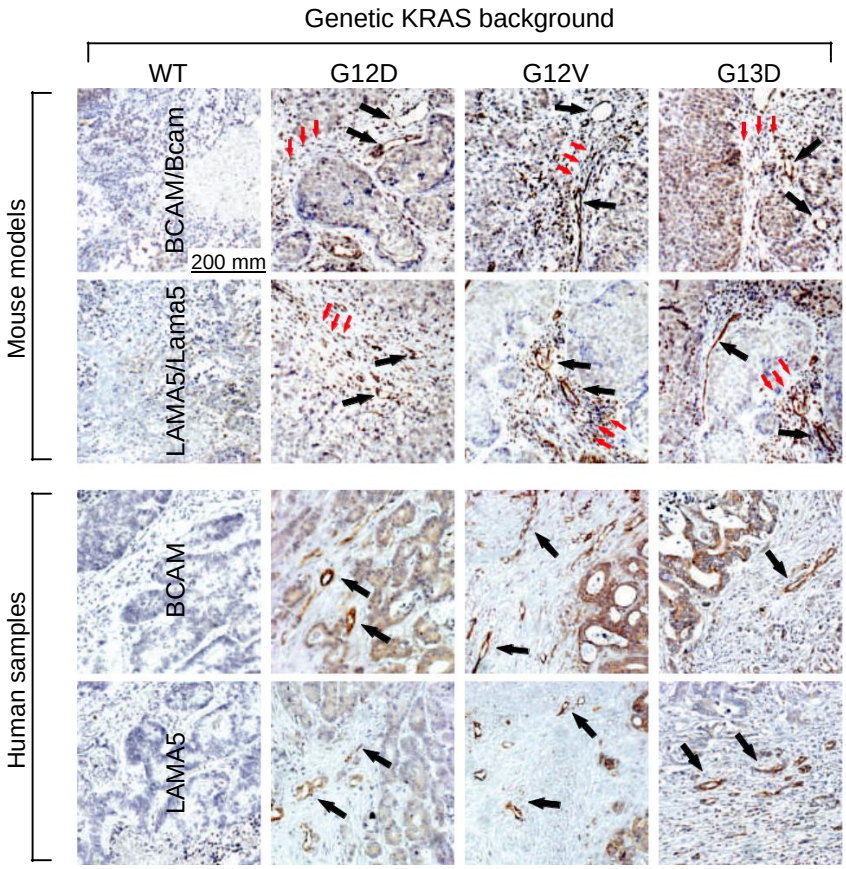

Bartolini et al_Fig3

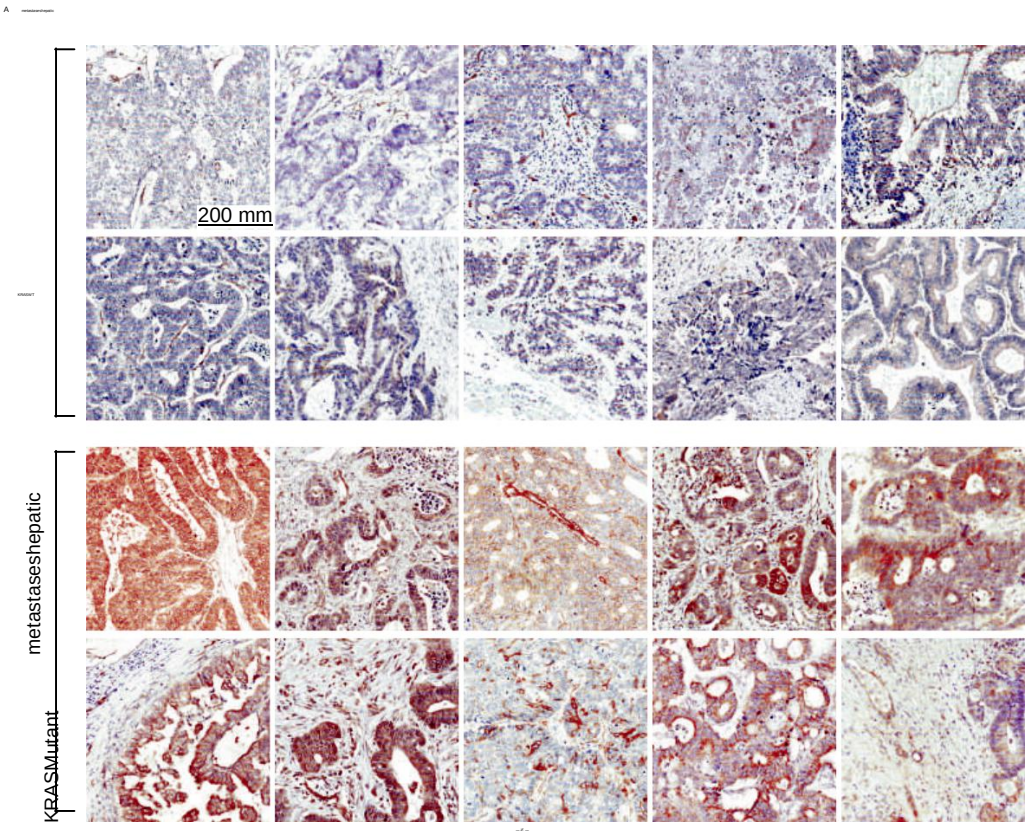

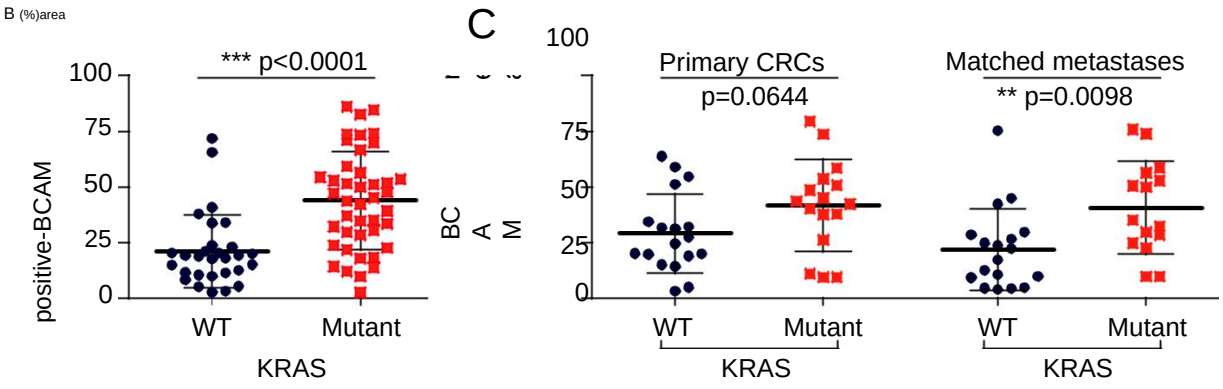

Bartolini et al_Fig4

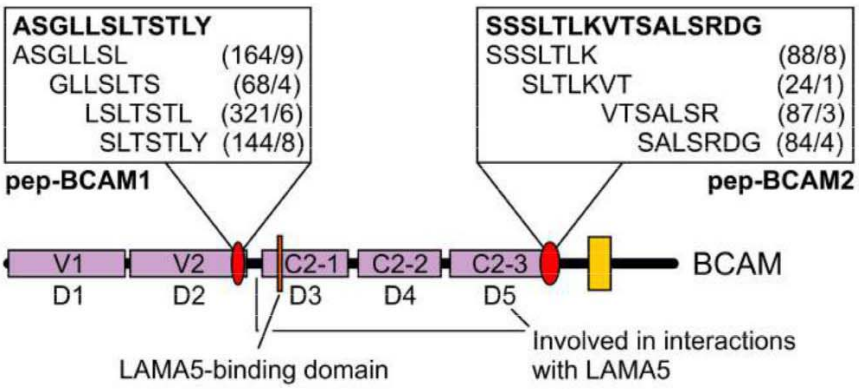

Bartolini et al_Fig5

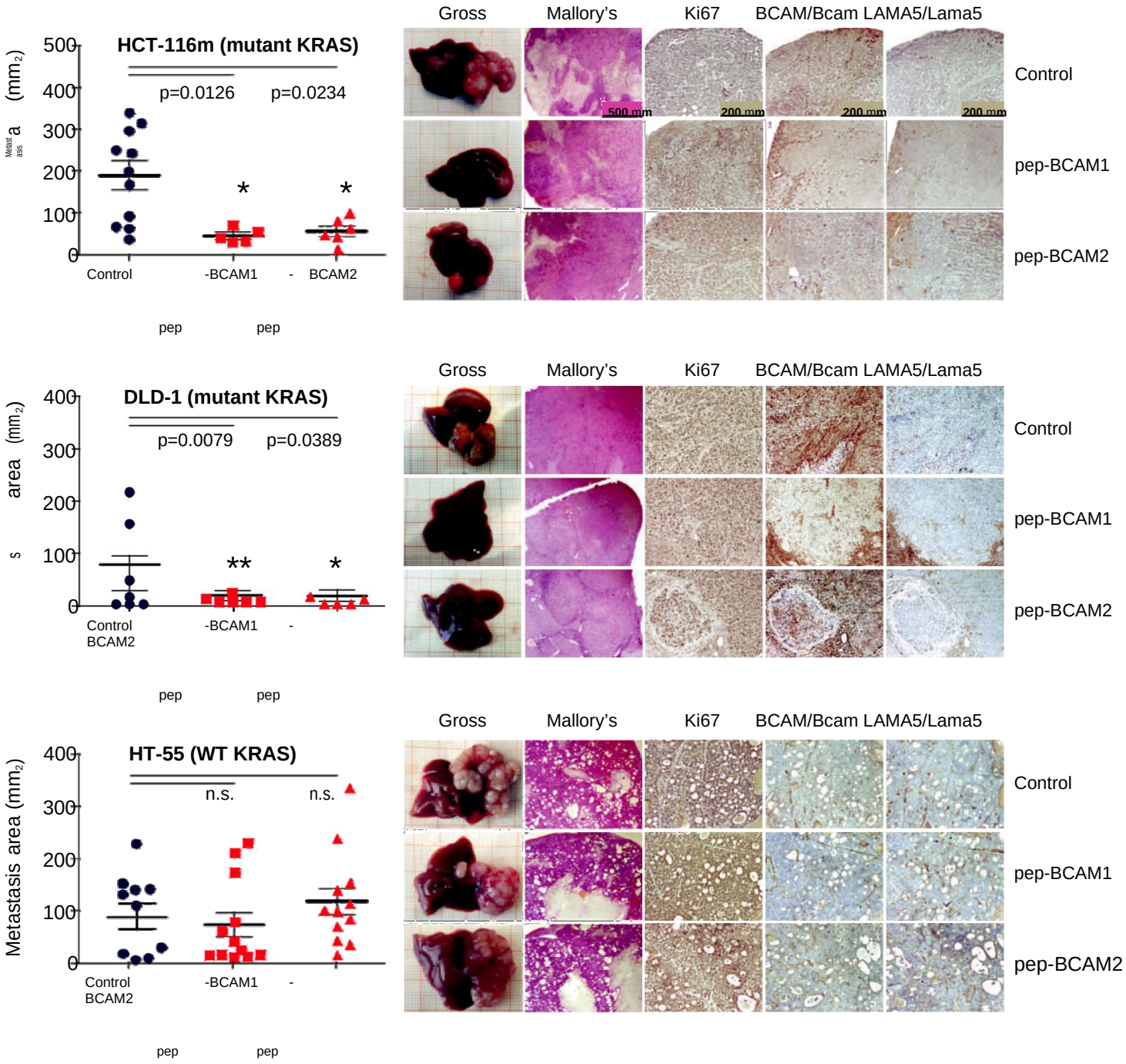

Bartolini et al_Fig6